Available online at www.sciencedirect.com

ScienceDirect

Physics Procedia 83 (2016) 1130 – 1136

Physics Procedia

9th International Conference on Photonic Technologies - LANE 2016

Effect of ultrashort pulse laser structuring of stainless steel on laser-based heat conduction joining of polyamide steel hybrids

Philipp Amend[a,*], Tom Häfner[b,c], Michael Gränitz[a], Stephan Roth[a,c], Michael Schmidt[a,b,c]

[a]*Bayerisches Laserzentrum GmbH (blz), Konrad-Zuse-Straße 2-6, 91052 Erlangen, Germany*
[b]*Institute of Photonic Technologies (LPT), Friedrich-Alexander-Universität Erlangen-Nürnberg, Konrad-Zuse-Straße 3-5, 91052 Erlangen, Germany*
[c]*Erlangen Graduate School in Advanced Optical Technologies (SAOT), Paul-Gordan-Straße 6, 91052 Erlangen, Germany*

Abstract

The objective of this paper is to investigate how microstructures generated by ultrashort pulse laser structuring of stainless steel affect the laser-based joining of thermoplastic metal hybrids. For structuring experiments a picosecond laser (λ = 1064 nm) is used. The machined surfaces are topographically analyzed by optical microscopy. The experimental setup for the joining process consists of a disk laser (λ = 1030 nm), a scanner optic and a clamping device for lap joint. The joined specimens are mechanically analyzed by tensile shear tests and the influence of ultrashort pulse laser structuring on the mechanical properties of the dissimilar joints is evaluated. Besides, a fracture analysis of the mechanically tested specimens using scanning electron microscope (SEM) images and energy dispersive X-ray spectroscopy (EDX) mapping is done.

Peer-review under responsibility of the Bayerisches Laserzentrum GmbH

Keywords: ultrashort pulse laser structuring; laser-based heat conduction joining; polyamide steel hybrid

1. Introduction and approach

During the last years, several studies have been conducted to improve the laser-based joining of thermoplastic metal hybrids. A lot of scientists including the author tried to improve the joint quality by a prior laser surface enlargement of the metallic joining partner using a continuous wave fiber laser or a pulsed nanosecond laser (e. g.

* Corresponding author. Tel.: +49-9131-997790-28 ; fax: +49-9131-997790-11 .
E-mail address: p.amend@blz.org

Peer-review under responsibility of the Bayerisches Laserzentrum GmbH
doi:10.1016/j.phpro.2016.08.118

Amend et al. (2013), Rodríguez-Vidal et al. (2014), Rösner (2015)) in order to achieve macroscopic surface structures for a strong mechanical interlocking. Thereby, tensile shear strengths in the range of 15 and 20 MPa (e. g. Engelmann et al. (2013), Amend et al. (2015)) are typically reached. Only a few scientists (e. g. Engelmann et al. (2015), Heckert et al. (2015)) reported values between 20 and 25 MPa.

Promising studies on nano- and microstructuring of the surface for high-strength hybrid joints (Kurtovic et al. (2013), Kurtovic (2014)) already exist for adhesive bonding with chemically reactive adhesives. However, up to now there is a lack of knowledge of how microstructures generated by ultrashort pulse laser structuring of metal affect the laser-based joining of thermoplastic metal hybrids. That is why in this paper experimental investigations of laser-based heat conduction joining with prior ultrashort pulse laser structuring of stainless steel are presented.

2. Materials and experimental setup

2.1. Materials

For the experiments, stainless steel (1.4301, 50 mm · 50 mm · 1 mm) and unfilled polyamide 6 (PA6, TECAMID 6, 50 mm · 50 mm · 2 mm) are used. Four polyamid specimens are analyzed by Karl-Fischer-Titration and a mean moisture content of 2.019 ± 0.148 wt.-% is detected. The stainless steel has a 2B surface finish that means that the sheet is cold-rolled and subsequently finished by annealing, etching and cold re-rolling. To remove contaminants from the surface, metal samples are cleaned in an ultrasonic water bath and with acetone. The PA6 specimens are solely cleaned with acetone because polyamide is hygroscopic.

2.2. Laser structuring

The stainless steel is structured with an ultrashort pulse laser with the pulse duration $t_p = 10$ ps and the wavelength $\lambda = 1064$ nm. For the experiments, a repetition rate of $f_P = 200$ kHz and a beam diameter of about d = 60 µm are used. Further relevant laser structuring parameters are shown in Tab. 1. The deflection of the gaussian beam is realized by a galvano scanner and a f-theta objective with f = 160 mm. The pre-treatment is performed to investigate how microstructures generated by ultrashort pulse laser structuring affect the laser-based joining of thermoplastic metal hybrids. Thereby, the influence of structure width and structure arrangement as well as surface roughness and surface enlargement are analyzed. The laser parameters are chosen based on preliminary experiments so that a smooth structure (A) and a rough structure (B) with a significantly increased surface area are produced. All experiments are carried out in air under ambient pressure.

Table 1. Laser structuring parameters.

Surface type	Average laser power P_a [W]	Pulse energy E_p [µJ]	Scan velocity v_s [mm/s]	Number of scans n_s [-]	Hatch distance h_y [µm]
Structure A	22.9	114.5	1200	7	15
Structure B	11.3	14.3	50	1	7.5

2.3. Laser-based joining

In this paper, an experimental setup consisting of a disk laser ($\lambda = 1030$ nm), a scanner optic and a clamping device for lap joint are used to join thermoplastic metal hybrids. During the joining, the velocity is varied between 40 and 60 mm/s, whereas the laser power P = 1000 W and the beam diameter d = 6 mm are kept constant. For the joining process, the specimens are fixed in overlap configuration (contact area $A_c = 1000$ mm^2) by means of a clamping device and joined under pressure ($p_{join} = 2$ MPa). For this joining technique no adhesive is needed and the adhesion between the dissimilar materials is based on a direct thermal-induced physically bonding of the thermoplastic part to the metallic surface. During the laser-based joining of thermoplastic metal hybrids, the laser radiation is absorbed by the stainless steel surface which leads to an increase of the material temperature. Positioned below the metal, the thermoplastic melts as a result of heat transfer. The thermoplastic melt wets the metal surface which is solely cleaned or laser-structured. After cooling, the dissimilar materials are joined together.

2.4. Surface analysis and testing of joined polyamide steel hybrids

The machined surfaces are topographically analyzed by laser scanning microscopy (LSM), whereby the average mean roughness S_a aaccording to DIN EN ISO 25178 and the surface enlargement S_E are measured. To determine the increase in surface area, there is no standardized procedure. For this work, the LSM images of the surfaces are taken with a magnification of 20, whereby the real surface areas are measured. Afterwards, the surface enlargement S_E can then be determined from the ratio of measured surface and the geometric, ideal surface.

The joined specimens are visually characterized by means of a desk scanner and subsequent image processing to analyze the wetting area A_w. After that, the breaking force F_{break} of the hybrid is analyzed by tensile shear test. Based on these experiments, the tensile shear strength τ is calculated by the quotient of measured breaking force F_{break} and measured wetting area A_w. Finally, the fracture behavior is analyzed by scanning electron microscope (SEM) images and energy dispersive X-ray spectroscopy (EDX) mapping.

3. Results and discussion

3.1. Influence of laser structuring on the surface topography

In Fig. 1 the average mean roughness S_a and the surface enlargement S_E as well as top-view SEM images of untreated and ultrashort pulse laser-structured stainless steel surfaces are shown. It can be stated that the untreated and the surface with structure A have a smooth surface, whereas the surface with structure B is rough and significantly enlarged by the laser structuring process. It also can be seen that the surface topography (see Fig. 1(b)). has changed from a characteristic 2B finished stainless steel surface to a surface consisting of microcones and nanoripples (see Liu et al (2013)).

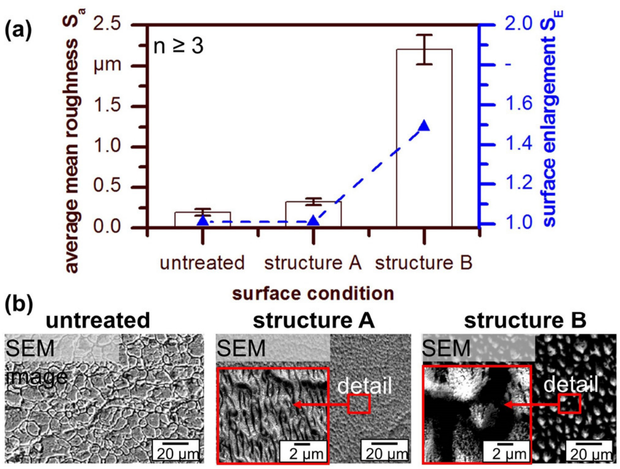

Fig. 1. (a) Average mean roughness S_a and surface enlargement S_E for untreated and ultrashort pulse laser-structured stainless steel; (b) SEM images of untreated and ultrashort pulse laser-structured stainless steel.

3.2. Influence of structure width and its arrangement

First of all, the influences of structure width and its arrangement on the tensile shear strengths of the hybrids are investigated. Therefore, samples are generated with structure B, whereby the structure width is varied between 1.0 and 3.0 mm. After that, all specimens are joined with PA6 using the parameters P = 1000 W, v = 60 mm/s, d = 6 mm (see Fig. 2(a)) and are mechanically tested by tensile shear tests. As reference untreated specimens are joined and tested, too. The results of the tensile shear tests are shown in Fig. 2(b). It has to be mentioned that the wetting width w (see Fig. 2(a)) for the used joining parameter is about 3.9 mm so that all created structure widths s are wetted by polymer melt during laser-based joining. However, surface areas which are directly bonded to the untreated stainless steel exist, too. The distribution of bonding to an untreated or a laser-structured surface depends on the used structure width. According to Fig. 2(b) it can clearly stated that with increasing structure width and constant wetting width the tensile shear strength nearly linearly increases. The tensile shear strength is more then quadrupled for a structure width s of 3.0 mm in contrast to solely cleaned specimens. To achieve a very high tensile shear strength, for the following experiments only structure width s = 3.0 mm is used.

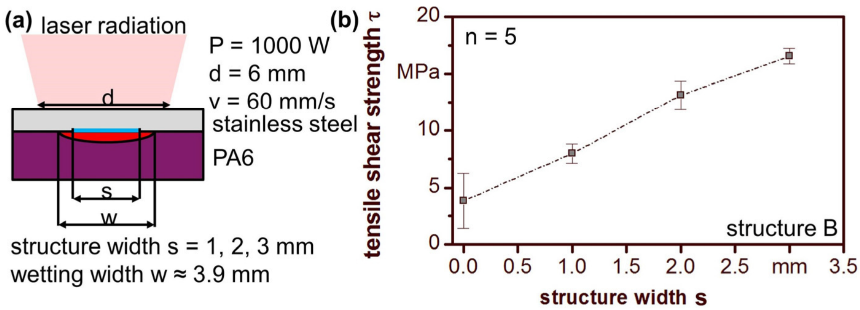

Fig. 2. (a) Schematic illustration of experimental setup for laser joining of the specimens used for tensile shear tests;
(b) Tensile shear strength τ for laser-based joined hybrids with ultrashort pulse laser-structured stainless steel with varied structure width s.

In the next step, the structure arrangement is analyzed. Thereby, the sum of structure width s = 3 is kept constant and only the arrangement is varied. Therefore, the following structure arrangements are realized and joined with the parameters P = 1000W, v = 60 mm/s, d = 6 mm: $a_1 = 1 \cdot 3.0$ mm, $a_2 = 2 \cdot 1.5$ mm and $a_3 = 3 \cdot 1.0$ mm (see Fig. 3(a)). It can be stated that the structure arrangement a has no measurable impact on the tensile shear strength if the sum of structure width is equal. It does not matter whether there is one structured area with a structure width of s = 3 mm ($a_1 = 1 \cdot 3$ mm) or several structured areas of various widths (see Fig. 3(a); $a_2 = 2 \cdot 1.5$ mm; $a_3 = 3 \cdot 1.0$ mm). Furthermore, the experiments show that the tensile shear strength depends on the surface structure type. Soley cleaned metallic samples that are joined with the parameters P = 1000W, v = 60 mm/s, d = 6 mm to PA6 reach tensile shear strengths of just below 4 MPa (see Fig 2(b) and 3(b)). Specimens that are pre-treated with a ultrashort pulse laser and joined with comparable parameters achieve values of 12 to 13 MPa for structure A and 16 to 17 MPa for structure B. The influence of the surface structure type of the metal on the hybrid joint property is discussed in detail in the next section.

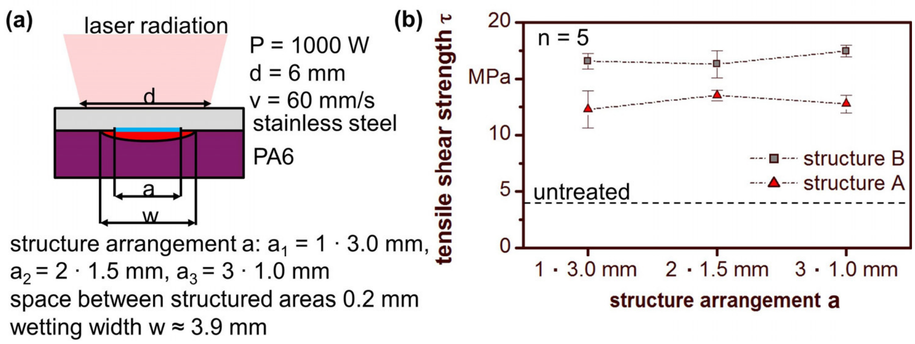

Fig. 3. (a) Schematic illustration of experimental setup for joining the specimens used for tensile shear tests;
(b) Tensile shear strength τ for laser-based joined hybrids hybrids with ultrashort pulse laser-structured stainless steel whereby the structure arrangement is varied for structure A and B and the results are compared to the tensile shear strength of hybrids with untreated metals.

3.3. Influence of structure type and joining parameters

Technical surfaces are not ideal surfaces and have a characteristisc topography and morphology. The topography describes the surface from a purely geometrical point of view, whereas the morphology takes the chemical layer constitution into account. In this paper, austentic stainless steel (1.4301) with a typical chromium content of about 18 wt.% is used. The chromium contained in stainless steel is mainly responsible for corrosion resistance. Chromium oxidizes faster than iron and it forms a closed nanoscale oxide layer on the steel surface (Henkel et al. (2008)). The outer layer of the passive layer consists of hydroxides (OH) and oxyhroxides (OOH) of iron and chromium (Schmucki et al. (2001)).

Although numerous studies have been conducted to determine the fundamental reasons for adhesion between interfaces, until today the exact causes are still not clarified (Habenicht (2009)). In respect to the investigation for joining polyamide steel hybrids, the authors assume based on literature (see Bischof et al (1982)) that mechanical and specific adhesion play an important role. Especially dipole interactions, hydrogen bonds and dispersion forces that can be formed between the amino (NH), methyl (CH_2) and carbonyl (CO) groups of polyamide and the oxygen containing interface (oxide, (oxy)hydroxide) of the stainless steel appear to induce adhesion. Moreover, some authors report that chemisorption between metal and plastic can take place.

From this viewpoint, it is important to take into account that a laser surface pre-treatment inevitably changes the surface topography as well as the surface morphology. The change in the surface morphology is determined primarily by oxidation processes (Adams et al. (2013)) whereby among others Cr_2O_3 and Fe_2O_3 are formed (Cui et al. (2014)). The surface topography can be modified in various ways. In this paper, two laser structured surfaces types are considered which differ in surface roughness and surface area (see Fig. 1(a) and (b)). The smooth surface (structure A) which has a low average mean roughness S_a of 0.32 µm is generated by multiple scanning ($n_s = 7$) of the surface with a high scanning velocity ($v_s = 1200$ mm/s) and a relatively high pulse energy (E_p = 114.5 µJ) (further parameters, see Tab. 1). According to the LSM measurements the surface area is almost not increased in comparison to the reference material. However, in the SEM image (see Fig. 1(b), structure A) a periodic porous texture can be seen which might indicate nanoripples and may improve adhesion. The rough surface (structure B) which is generated by a single pass ($n_s = 1$) with a low scan velocity ($v_s = 50$ mm/s) and a moderate pulse energy (E_p = 14.3 µJ) has an average mean surface S_a 2.2 µm and its surface is enlarged by the factor of 1.5. The enlargement of the surface can be explained primarily by the laser-induced formation of microcones (see Fig. 1 (b), structure B).

In contrast to the preliminery joining experiments, for these investigations the joining velocity is varied in the range of 40 and 60 mm/s to consider the effect of energy input and the directly related bonding temperature on the mechanical properties of the joint. First of all, it can be noted that the tensile shear strength depends significantly on surface pretreament. Prior to further discussion, it must be pointed out once again that the structure width is kept constant even if different joining velocities are used which lead to different wetting widths (see Fig. 4(a)). Therefore, the percentage of wetting area A_w which is untreated increases with decreasing joining velocity. Although almost the entire wetting area A_w joined by the parameters P = 1000 W, d = 6 mm, v = 60 mm/s is laser-structured, the highest tensile shear strength is reached for the velocity v = 50 mm/s. This can be explained by the fact that a higher bonding temperature in the interface between thermoplastic and metal ,respectively, a longer wetting time are achieved for a lower joining velocities. Further information about the process-structure-property relationship of laser-joined thermoplastic metal hybrids can be found by Amend et al. (2016). The decrease in tensile shear strength for a joining velocity of 40 mm/s can be attributed to the increasing percentage of unstructured surface. Thus, it can not be answered which are the final optimum joining parameters. However, it can be clearly seen that the untreated surface always has the lowest adhesion.

Regarding the tensile shear strengths which are achieved in laser-based joining of thermoplastic metal hybrids with a prior laser surface enlargement of the metallic joining partner using a continuous wave fiber laser or a pulsed nanosecond laser, the tensile shear strengths τ are subdivided into strong joints (τ_{strong} = 15 - 20 MPa) and extreme strong joints ($\tau_{extreme\ strong}$ = 20 - 25 MPa) (see Fig. 4(b)). It turns out that the smooth structure A reach values just below or above the limit for strong joints, whereas the rough surface B always at least reach values above this limit. Even extreme strong joints with tensile shear strength up to 23 MPa are obtained for structure B (see Fig. 4(b)).

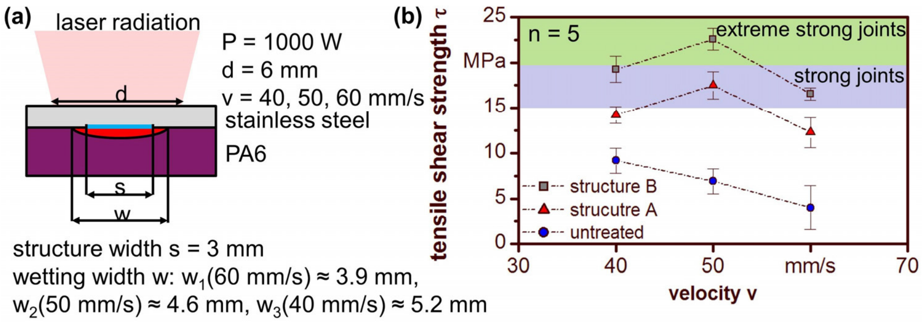

Fig. 4. (a) Schematic illustration of experimental setup for joining the specimens used for tensile shear tests;
(b) Tensile shear strength τ for laser-based joined hybrids hybrids with ultrashort pulse laser-structured stainless steel wherby the structure width is 3.0 mm and the wetting width w is varied based on the joining velocity for structure A and B. The results are compared to tensile shear strengths of hybrids with untreated metals.

The analysis of fracture behavior gives further informations on the adhesion between PA6 and stainless steel. In Fig. 5 a schematic illustration of the fracture analysis is shown. The analyzed sample has two laser-structured areas (structure A and B, see Fig. 5(a) and (b)) and is joined with the laser parameters P = 1000W, v = 40 mm/s, d = 6 mm. The wetting area A_w, respectively, the wetting width w are also shown schematically in Fig. 5. In addition, two areas are marked where SEM images are taken. For a better understanding of the fracture behavior EDX mappings of selected areas are performed to determine the elemental composition of the surface, too. Therefore, it must be mentioned that PA6 consists of 63.7 wt.% carbon (Becker et al. (1998)), so that the element carbon represents PA6 in EDX mapping images (see Fig. 5 (a) and (b)). The analysis of the surface A shows that there is an adhesive failure in the joining zone and almost no PA6 remains on the metallic surface. There are only some residues on the edge of the joining zone (see Fig. 5(a), EDX mapping). Due to the fact that the tensile shear strength is significantly increased for structure A in contrast to solely clean specimes with almost the same average mean roughness S_a and surface enlargement S_E it is believed that the improved adhesion is caused by the laser-induced oxidation of the surface as well as the periodic porous textures (see Fig. 1(b) structure A). The oxidation of the surface promotes, i.a., the formation of additional hydrogen bonds and dispersion forces between PA6 and steel, whereas the porous surface texture leads to a mechanical interlocking. The oxidation and microcones of structure B generated extreme strong joints. The fracture analysis for structure B shows that a cohesive failure of the thermoplastic material occurs (see Fig. 5 (b)). This means that a material-related maximum for the joint between PA6 and stainless steel is reached by ultrashort pulse laser structuring of stainless steel

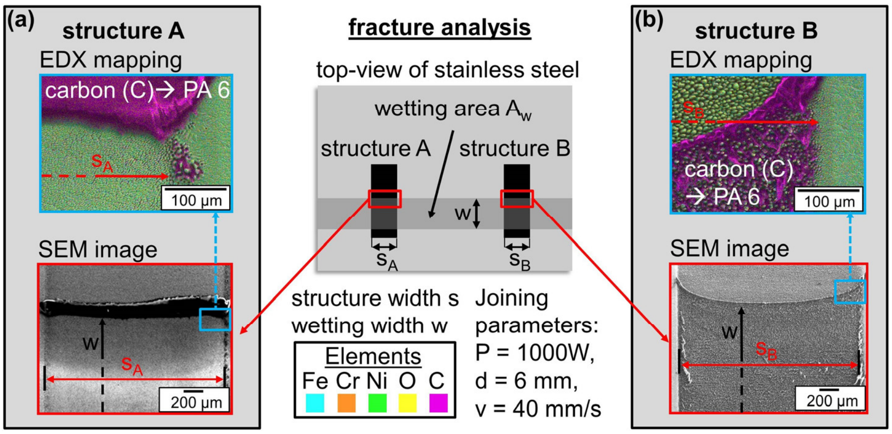

Fig. 5. Fracture analysis of a mechanically tested specimen using SEM images and EDX mappings for structure A (see (a)) and B (see (b)).

4. Summary and outlook

In this paper, the effect of ultrashort pulse laser structuring of stainless steel on laser-based heat conduction joining of polyamide steel hybrids is investigated. Therefore, experiments with varied structure width, arrangement and type are conducted. The structure width as well as the ratio of structure width and wetting width significantly influences the tensile shear strength, whereby the structure arrangement has no impact on the mechanical property of the joint if the sum of structure width is equal. According to experiments, it can clearly stated that the tensile shear strength directly depends on the surface structure type. It is assumend that joining of PA6 to stainless steel is caused by specific and mechanical adhesion. The conducted experiments demonstrate that the surface treatment of stainless steel with an ultrashort pulse laser leads to strong and extreme strong hyrid joints up to a cohesive failure in the base material of the polyamide 6. It is concluded that the improvement in adhesion can be attributed to the oxidation of the surface that enables further formation of adhesion forces (e.g. dipole interactions, hydrogen bonds and dispersion forces) and the porous surface structures with microcones that lead to a mechanical interlocking. In future, further investigations have to be done to understand the formation mechanism of the micro- and nanoscale topographies which lead to a surface enlargement S_E. Evaluation of the laser-induced oxidation and its effect on element distribution at the metallic interface in dependency of laser parameter and environmental conditions will show the influence of the morphology on the polyamide steel hybrids. Thereby, especially the influence of ambient air in contrast to pure oxygen atmosphere or other process gases should be considered.

Acknowledgements

This work was partially funded by the Bavarian State Ministry of Economic Affairs and Media, Energy and Technology. The authors are grateful for the support.

References

Adams, D.P., Hodges, V.C., Hirschfeld, D. A., Rodriguez, M. A., McDonald, J. P., Kotula, P. G., 2013. Nanosecond pulsed laser irradiation of stainless steel 304L: Oxide growth and effects on underlying metal, Surface and Coatings Technology, Vol. 222.

Amend, P., Pfindel, S., Schmidt, M., 2013. Thermal joining of thermoplastic metal hybrids by means of mono- and polychromatic radiation, Physics Procedia, Vol. 41, pp. 98-105.

Amend, P., Hentschel, O., Machui, J., Scheitler, C., Roth, S., Schmidt, M., 2015. Effect of surface structures on laser-based joining of thermoplastic metal hybrids. In: Proceedings of LAMP 2015, 26.05.-29.05.2015, Kitakyushu, Fukuoka, Japan.

Amend, P., Mallmann, G., Roth, S., Schmitt, R., Schmidt, M., 2016. Process - structure - property relationship of laser-joined thermoplastic metal hybrids. J. Laser Appl., Vol. 28, No. 2.

Becker, G. W., Braun, D., Bottenbruch, L., Binsack, R., 1998. Polyamide. Kunststoff-Handbuch 3/4. Technische Thermoplaste. Hanser, 1998.

Bischof, C., Possart, W., 1982. Adhäsion. Theoretische und experimentelle Grundlagen. Akademie-Verlag.

Cui, Y.C., Cui, X.G., Ren, X.D., Qi, M.J., Hu, J.D., Wang, Y.M., 2014. Surface oxidation phenomenon and mechanism of AISI 304 stainless steel induced by Nd:YAG pulsed laser. Appl. Surf. Sc., Vol. 305.

Engelmann, C., Rösner, A., Olowinsky, A., Mamuschkin, V. 2013. Mikrostrukturen zum lasergestützten Fügen von Kunststoff und Metall. In: Große Schweißtechnische Tagung, DVS Congress 2013, 16.09.-21.09.2013, Essen, Germany.

Engelmann, C., Eckstädt, J., Olowinsky, A., Aden, M., Mamuschkin, V., 2015. Examination of the bond strength of laser assisted plastic-metal-joints considering different load directions. In: Proceedings of LAMP 2015, 26.05.-29.05.2015, Kitakyushu, Fukuoka, Japan.

Habenicht, G., 2009. Applied Adhesive Bonding. Wiley.

Heckert, A., Singer, C., Zaeh, M.F., 2015. Pulsed laser surface pre-treatment of aluminium to join aluminium-thermoplastic hybrid parts. In: Proceedings of LiM 2015. 22.06.-25.06.2015, Munich, Germany.

Henkel, G., Rau, J., Henkel, B., 2008. Topographie und Morphologie funktionaler Edelstahloberflächen. Expert Verlag.

Kurtovic, A.; Eiselen, S.; Amend, P.; Mertens, T.; Maier, H.J.; Schmidt, M., 2013. Laserinduzierte Nano- und Mikrostrukturierung von Titan- und Aluminiumlegierungen für hochwertige Klebeverbindungen. In: Tagungsband 16. LEF Seminar, S. 205-218, Meisenbach Verlag.

Kurtovic, A., 2014. Laserinduzierte Nanostrukturierung von Titanoberflächen für das strukturelle Kleben: Einfluss auf die Oberflächenmorphologie, Ermüdungs- und Adhäsionseigenschaften. Ph.D. thesis, University of Paderborn.

Liu, B., Wang, W., Jiang, G., Mei, X., Wang, K., J., 2013. Formation of porous structure with subspot size under the irradiation of picosecond laser pulses. J. of Nanomat.. Vol. 2013, Article ID 301301.

E. Rodríguez-Vidal, E. Rodríguez-Vidal, E., J. Lambarri, J., Soriano, C., Sanz, C., Verhaeghe, G., 2014. A Combined experimental and numerical approach to the laser joining of hybrid polymer – metal parts. Physics Procedia. Vol. 56, pp. 835-844.

Rösner, A., 2014. Laserbasiertes Fügeverfahren zur Herstellung von Kunststoff-Metall-Hybridbauteile. Ph.D. thesis, Fraunhofer Institute for Laser Technology ILT.